Available online at ScienceDirect

ScienceDirect

J. Mater. Sci. Technol., 2014, 30(1), 65−76

JMST

www.JMST.org

Effect of Hydrodynamic Conditions on Corrosion Inhibition of Cu−Ni (90/10) Alloy in Seawater and Sulphide Containing Seawater Using 1,2,3-Benzotriazole

B.V. Appa Rao[*], *K. Chaitanya Kumar*

Department of Chemistry, National Institute of Technology Warangal, Warangal, 506 004 Andhra Pradesh, India

[Manuscript received January 23, 2013, in revised form May 11, 2013, Available online 3 September 2013]

Electrochemical studies of the effect of hydrodynamic conditions on corrosion inhibition of Cu−Ni (90/10) alloy in synthetic seawater and sulphide containing synthetic seawater by 1,2,3-benzotriazole (BTAH) are presented. Impedance, potentiodynamic polarization and cyclic voltammetric (CV) studies are employed in the present investigation. The studies are carried out by using Cu−Ni (90/10) alloy rotating disc electrode at different rotation speeds and at different immersion periods. Reynolds numbers at each rotation speed infer that the flow of seawater is laminar. With increasing rotation speed of the electrode immersed in seawater without sulphide and BTAH, both the charge transfer resistance (R_{ct}) and film resistance (R_{film}) are increased. However, in the presence of sulphide ions and without BTAH, both the R_{ct} and R_{film} are found to decrease with increasing rotation speed at identical immersion periods. Interestingly, when BTAH is added to seawater or seawater containing sulphide, both the R_{ct} and R_{film} are increased to such a great extent that an inhibition efficiency of 99.99% is obtained. In the presence of BTAH, the phase angle Bode plots are more broadened and the maximum values of phase angle are increased to a value close to 90° as the rotation speed is increased. The BTAH film is highly protective even under hydrodynamic condition also. Potentiodynamic polarization studies infer that BTAH functions as a mixed inhibitor under hydrodynamic conditions also. CV studies reveal that the protective BTAH film is stable even at anodic potentials of +850 mV *vs* Ag/AgCl.

KEY WORDS: Cu−Ni (90/10) alloy; Rotating disc electrode; Seawater; Corrosion inhibition; Electrochemical studies; 1,2,3-Benzotriazole

1. Introduction

The Cu−Ni (90/10) alloy is known to have good resistance to both corrosion and biofouling in seawater. Hence, this alloy is the material of choice for seawater pipe work and condenser service for many of the world's navies and merchant ships[1−3]. The corrosion resistance of Cu−Ni (90/10) alloy is related to the performance of the passive film, Cu_2O[4−6]. However, in the sulphide-polluted seawater, the corrosion resistance is decreased because sulphide ions interfere with Cu_2O film formation and produce a non-protective black layer of Cu_2S[7−9]. Due to the passivation in seawater, the Cu−Ni (90/10) alloy shows higher corrosion resistance under flowing conditions than stagnant condition[10−15]. Eventhough, it has higher corrosion resistance under hydrodynamic condition, the corrosion resistance is decreased under longer exposure in seawater[16]. A few researchers have studied the effect of hydrodynamic condition on the corrosion behaviour of Cu−Ni (90/10) alloy in different aggressive environments. Kear et al.[17] studied the corrosion behaviour of Cu−Ni (90/10) alloy rotating disc electrode in both seawater and NaCl environments by employing potentiodynamic polarization and cyclic voltammetric (CV) studies. Hurtado et al.[18] investigated the electrochemical corrosion behaviour of Cu−5Ni rotating disc electrode in 0.5 mol/L H_2SO_4 solution by using open circuit potential (E_{OCP}) measurements, CV, electrochemical impedance studies, quasi-stationary linear potential sweep and surface examination by SEM−EDX. The dissolution of Cu−Ni (90/10) alloy in HCl at different concentrations under hydrodynamic conditions was studied by Walton and Brook[19]. They have employed potentiodynamic sweep and steady-state potential measurements on Cu−Ni (90/10) alloy rotating disc electrode. Nevertheless, no studies have been reported on corrosion behaviour of Cu−Ni (90/10) alloy in seawater and seawater containing sulphide under hydrodynamic conditions in the presence of an inhibitor. Hence, it is of interest to investigate the effect of hydrodynamic condition on corrosion inhibition of Cu−Ni (90/10) alloy in seawater and seawater containing sulphide by using 1,2,3-benzotriazole (BTAH). BTAH is chosen as the inhibitor for the following reasons. BTAH is well known corrosion inhibitor for

* Corresponding author. Prof., Ph.D.; Tel.: +91 870 2462652; E-mail address: boyapativapparao@rediffmail.com (B.V. Appa Rao).

http://dx.doi.org/10.1016/j.jmst.2013.08.019

Table 1 Composition of the Cu−Ni (90/10) alloy (wt%)

Cu	Ni	Fe	Mn	Pb	Al	Others in trace amounts
8.512	9.882	1.086	0.412	0.046	0.038	0.024

copper and its alloys. Babic et al.[20] studied the corrosion inhibition of Cu−Ni (90/10) alloy in 1 mol/L sodium acetate solution by using BTAH as inhibitor by employing CV, photopotential measurements and impedance studies under static conditions. Allam et al.[21] studied the inhibiting effect of benzotriazole on the corrosion of Cu−Ni (90/10) alloy in 3.4% NaCl solution containing 2×10^{-6} of sulphide ions under static conditions by weight-loss measurements and X-ray diffraction technique. Maciel and Agostinho[22] employed the potentiodynamic polarization studies on Cu−Ni (90/10) alloy rotating disc electrode in 0.5 mol/L H_2SO_4 solution containing Fe (III) ions as oxidant and BTAH as inhibitor. The authors of the present study reported good performance of BTAH as inhibitor through electrochemical investigations of Cu−Ni (90/10) alloy in seawater and sulphide-polluted seawater under static conditions[23]. The authors extended their studies further to investigate the inhibitor performance of benzotriazole under hydrodynamic conditions. A comprehensive study by employing electrochemical impedance, potentiodynamic polarization and CV studies on corrosion inhibition of Cu−Ni (90/10) alloy rotating disc electrode in synthetic seawater and sulphide containing synthetic seawater by 1,2,3-benzotriazole at different rotation speeds and immersion periods has been attempted in the present work.

2. Experimental

2.1. Materials

The composition of Cu−Ni (90/10) alloy used in the present study is given in Table 1. The synthetic seawater used in all the experiments is prepared by the composition given in Table 2[24]. All the chemicals used in the preparation of synthetic seawater were of AnalaR grade. A stock solution of 1000×10^{-6} of inorganic sulphide in synthetic seawater was first prepared. From this stock solution, 10×10^{-6} of sulphide containing seawater was prepared. 1,2,3-Benzotriazole obtained from Sigma−Aldrich was used as such. The Cu−Ni (90/10) alloy rotating disc electrode, purchased from Bioanalytical systems, USA, was used. This electrode was polished to mirror finish with alumina and water slurry on the micro polishing cloth, which is fixed on the rotating disc polishing machine. Then, the electrode was washed with triple distilled water, degreased with acetone and dried by blowing N_2 gas for 20 min.

2.2. Electrochemical studies

Electrochemical impedance studies were carried out in a three-electrode cell assembly (in accordance with ASTM specifications) by using an electrochemical work station, model IM6e Zahner elektrik, Germany. The Cu−Ni (90/10) alloy rotating disc electrode of the surface area of 0.07 cm^2 was used as the working electrode in the absence and presence of BTAH in seawater and sulphide containing seawater environments. The impedance values are normalized to the surface area of 1 cm^2. The impedance studies were carried out at 0, 1000 and 2200 r/min at identical immersion periods in the range of 1−48 h. A platinum electrode was used as the counter electrode and the reference electrode was Ag/AgCl/1.0 mol/L KCl electrode. The impedance studies were carried out at the open circuit potential (OCP) in the frequency range from 60 kHz to 10 mHz under excitation of sinusoidal wave of ±5 mV amplitude.

The potentiodynamic polarization and cyclic voltammetric studies were carried out by using the same three-electrode cell assembly and the electrochemical work station as described under impedance studies. The potentiodynamic polarization studies were conducted in the potential range of −0.7 V to +0.7 V *vs* Ag/AgCl with a scan rate of 1 mV s^{-1}. The CV studies were carried out in the potential range of −1.0 V to +1.0 V *vs* Ag/AgCl with a sweep rate of 10 mV s^{-1}. Potentiodynamic polarization and cyclic voltammetric studies were carried out at 0 and 2200 r/min for 1 and 48 h immersion periods. All the experimental data obtained by potentiodynamic polarization and CV studies were normalized to the surface area of 1 cm^2.

Table 3 Reynolds number of Cu−Ni (90/10) alloy rotating disc electrode at each rotation speed

Rotation speed (r/min)	Reynolds number, Re
0	0
1000	225
2200	495

3. Results and Discussion

3.1. Reynolds number

Reynolds number is useful to determine whether the flow of seawater is laminar or turbulent. It is calculated from the value of rotation speed, which is in the range of 0 and 2200 r/min in the present studies. The Reynolds number (Re) is calculated at each rotation speed by using the Eq. (1).

$$\mathrm{Re} = \frac{r^2 w}{k_v} \quad (1)$$

where r, ω and k_v are the radius of the rotating disc electrode (RDE) in mm, angular velocity in rad s^{-1} and kinematic viscosity in stokes (mm^2/s), respectively. The Reynolds numbers are presented in Table 3 which shows that at all the rotation speeds, the flow of seawater is laminar only.

3.2. Electrochemical impedance studies

The authors of the present study reported that the optimum concentration of 1,2,3-benzotriazole is 3.33 mmol/L in order to inhibit general corrosion of Cu−Ni (90/10) alloy in seawater and

Table 2 Composition of the synthetic seawater (g/L)

NaCl	KCl	$MgCl_2 \cdot 6H_2O$	$CaCl_2$	$MgSO_4 \cdot 7H_2O$	$NaHCO_3$	KBr	H_3BO_3	$SrCl_2 \cdot 6H_2O$	NaF
27.24	1.40	10.11	2.28	13.92	0.39	0.20	0.026	0.04	0.006

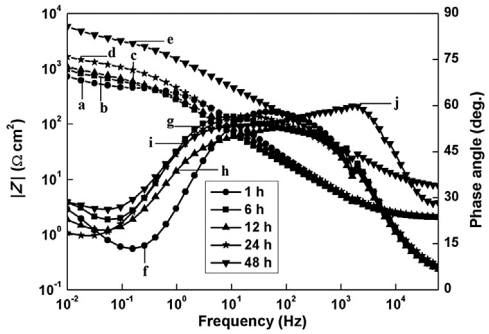

Fig. 1 Bode plots of Cu−Ni (90/10) alloy in seawater in the absence of BTAH at 0 r/min and at different immersion periods (temperature: 30 °C). a, b, c, d, e—frequency−Z curves; f, g, h, i, j—frequency−phase angle curves.

seawater containing sulphide under static condition by using 4.0 cm × 1.0 cm × 0.2 cm alloy specimen and exposing 1 cm^2 surface area[23]. Therefore, 3.33 mmol/L concentration of BTAH is chosen in the present study in order to investigate the effect of hydrodynamic condition on inhibitor performance. Fig. 1 shows the Bode plots of Cu−Ni (90/10) alloy in seawater at 0 r/min and at different immersion periods in the absence of any inhibitor. It is evident from the plots that with increasing immersion period, there is broadening of the maximum of phase angle, with a shift towards higher frequency. These plots infer an increase in the protective nature of the film with increasing immersion period[14,25]. With increasing rotation speed of the working electrode to 1000 r/min, interesting features of Bode plots are observed as shown in Fig. 2. The $|Z|$ *vs* frequency plots are characterized by a very large linear range especially at the immersion periods ≥12 h. The phase angle *vs* frequency Bode plots at these immersion periods are characterized by very broad maxima with the maxima of phase angles being close to 85°. These features of Bode plots infer that with increasing rotation speed from 0 to 1000 r/min, the protective nature of the film is significantly increased. With increasing rotation speed, the oxygen transport towards metal surface is increased. Hence, Cu_2O film forms very quickly and also the surface coverage of the film is greater[17,26]. All the plots show two time constants. In order to account for the above results, the metal/solution interface is modelled as per the equivalent circuit shown in Fig. 3(a)[27], whereas, in the presence of inhibitor the equivalent circuit shown in Fig. 3(b) is used. The physical model is considered to be the

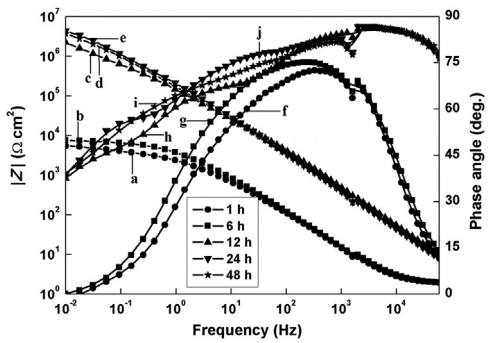

Fig. 2 Bode plots of Cu−Ni (90/10) alloy in seawater in the absence of BTAH at 1000 r/min and at different immersion periods (temperature: 30 °C). a, b, c, d, e—frequency−Z curves; f, g, h, i, j—frequency−phase angle curves.

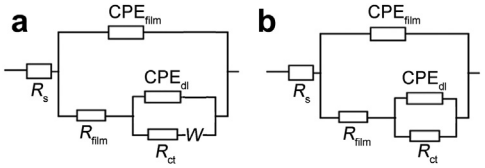

Fig. 3 Equivalent circuits used. R_{ct}—charge transfer resistance, R_s—solution resistance, R_{film}—film resistance, CPE_{film}—constant phase element of film, CPE_{dl}—constant phase element of double layer, W—Warburg impedance.

metal/protective surface film/electrical double layer/electrolyte solution. In this model, constant phase element (CPE) is introduced for the double layer capacitance (C_{dl}) to give a more accurate fit[28]. The admittance and impedance components of the CPE value are given in Eqs. (2) and (3), respectively.

$$Y_{CPE} = Y_0(j\omega)^n \quad (2)$$

$$Z_{CPE} = \frac{1}{Y_0(j\omega)^n} \quad (3)$$

where Y_0 is the magnitude of the CPE, j is the imaginary number, ω is the angular frequency[29]. The factor 'n' is the adjustable parameter that usually lies between 0 and 1[30]. The CPE describes an ideal capacitor when n is equal to 1[28,30]. The impedance parameters obtained with the fit shown in Fig. 3(a) are given in Table 4. The charge transfer resistance (R_{ct}) values are increased and CPE values are decreased with increasing rotation speed from 0 to 1000 r/min. With a further increase in rotation speed from 1000 to 2200 r/min, the maximum of phase angle is reduced from 85° to 75° at identical immersion periods, as shown in Fig. 4(a). It is interesting to note Warburg impedance in the Nyquist plots at lower immersion periods at all rotation speeds. As an example, the Nyquist plots at 2200 r/min only are shown in Fig. 4(b). Both the charge transfer resistance (R_{ct}) and film resistance (R_{film}) are decreased at 2200 r/min in comparison with 1000 r/min. But, these values are higher than the corresponding values at 0 r/min. All these results indicate that the protective nature of Cu_2O film is relatively decreased under higher rotation speeds. This is due to the increase in shear stress on the electrode with increasing rotation speed. This leads to the mass transport of Cu^+ ions from the electrode surface to the bulk of solution.

In the presence of 10×10^{-6} sulphide in seawater at 0 r/min (Fig. 5), the Bode plots exhibit different behaviours from the corresponding plots in seawater without sulphide (Fig. 1). The phase angle Bode plots reveal a decrease in the maximum of phase angle with increasing immersion period. The maximum of phase angle becomes narrow and decreases from 77° after 1 h immersion period to 47° after 48 h immersion period. The total impedance Bode plots also indicate a decrease in impedance values with increasing immersion period. The maximum of phase angle appeared at relatively much lower frequencies in comparison to seawater environment with no sulphide. Lower values of the maxima of phase angles and their appearance at lower frequency are attributed to the active pit growth on alloy surface due to the attack of S^{2-} ions[14]. The maxima of phase angles and impedance values are drastically reduced with increasing rotation speed from 0 to 2200 r/min. This is because of the adverse effect of sulphide ions present in seawater on Cu−Ni (90/10) alloy. Interestingly, after 24 and 48 h immersion periods, at both 1000 (Fig. 6) and 2200 r/min (Fig. 7(a)), the maxima of phase angles show two time constants very distinctly. The maximum of phase

Table 4 Impedance parameters of Cu−Ni (90/10) alloy electrode in seawater in the absence of BTAH at different hydrodynamic conditions and at different immersion periods (temperature: 30 °C)

Rotation speed (r/min)	Immersion period (h)	R_{ct} (kΩ cm^2)	CPE_{dl} (μF cm^{-2})	n_1	R_{film} (kΩ cm^2)	CPE_{film} (μF cm^{-2})	n_2
0	1	0.43	39.09	0.64	0.001	52.54	0.61
	6	0.72	35.71	0.67	0.001	49.31	0.62
	12	1.31	34.74	0.68	0.001	44.71	0.62
	24	2.34	15.44	0.69	0.002	32.75	0.63
	48	2.40	14.54	0.70	0.002	30.11	0.64
1000	1	4.20	7.16	0.64	0.320	12.84	0.63
	6	6.67	4.53	0.70	0.621	10.44	0.64
	12	108.6	0.33	0.72	37.28	0.39	0.65
	24	198.2	0.17	0.73	115.9	0.38	0.67
	48	220.0	0.16	0.77	146.7	0.36	0.67
2200	1	1.47	9.01	0.62	0.47	32.51	0.60
	6	1.75	7.69	0.67	0.71	19.27	0.67
	12	122.8	0.16	0.69	20.64	1.01	0.72
	24	128.0	0.15	0.70	27.36	1.00	0.73
	48	126.6	0.21	0.71	29.65	0.92	0.73

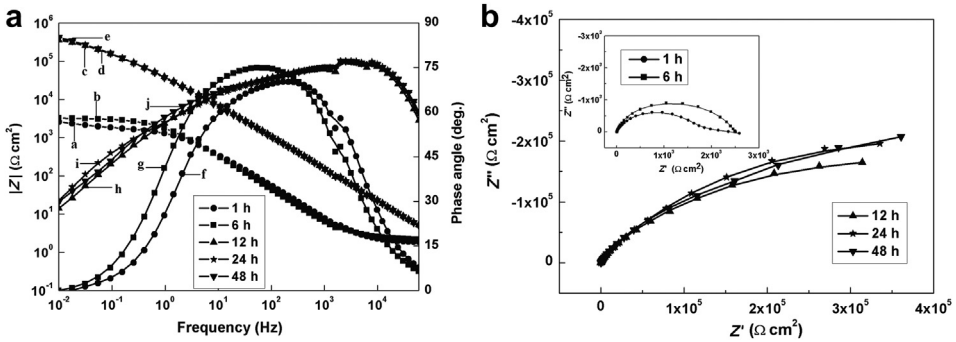

Fig. 4 (a) Bode and (b) Nyquist plots of Cu−Ni (90/10) alloy in seawater in the absence of BTAH at 2200 r/min and at different immersion periods (temperature: 30 °C). a, b, c, d, e—frequency−Z curves; f, g, h, i, j—frequency−phase angle curves.

angle at a lower frequency region is attributed to active pit growth and the maximum in the high frequency region is attributed to oxide film on alloy surface[31−35]. Warburg impedance was observed in Nyquist plots of Cu−Ni (90/10) alloy in sulphide containing seawater at all rotation speeds and at all immersion periods. As an example, the Nyquist plots at 2200 r/min only are given in Fig. 7(b). The experimental data are found to fit well with the same equivalent circuit model shown in Fig. 3(a) and the calculated impedance parameters are given in Table 5. The R_{ct} and R_{film} values are drastically reduced with increasing rotation speed. These values are far less than those obtained for the alloy immersed in seawater in the absence of sulphide ions. Both CPE_{dl} and CPE_{film} values are increased with increasing rotation speed as well as immersion period at each rotation speed.

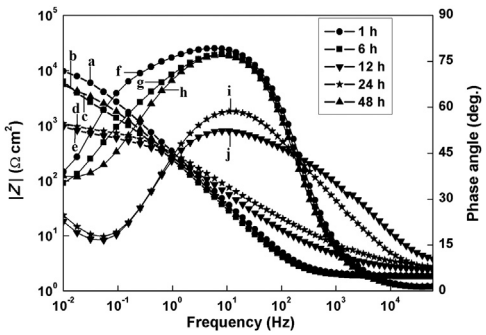

Fig. 5 Bode plots of Cu−Ni (90/10) alloy in seawater containing 10×10^{-6} sulphide in the absence of BTAH at 0 r/min and at different immersion periods (temperature: 30 °C). a, b, c, d, e—frequency−Z curves; f, g, h, i, j—frequency−phase angle curves.

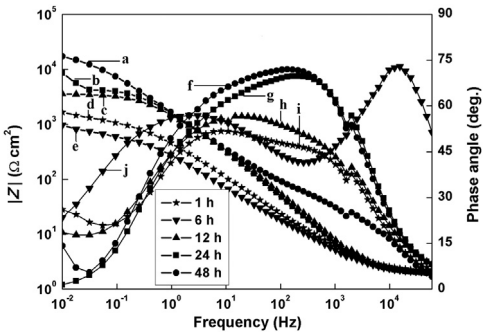

Fig. 6 Bode plots of Cu−Ni (90/10) alloy in seawater containing 10×10^{-6} sulphide in the absence of BTAH at 1000 r/min and at different immersion periods (temperature: 30 °C). a, b, c, d, e—frequency−Z curves; f, g, h, i, j—frequency−phase angle curves.

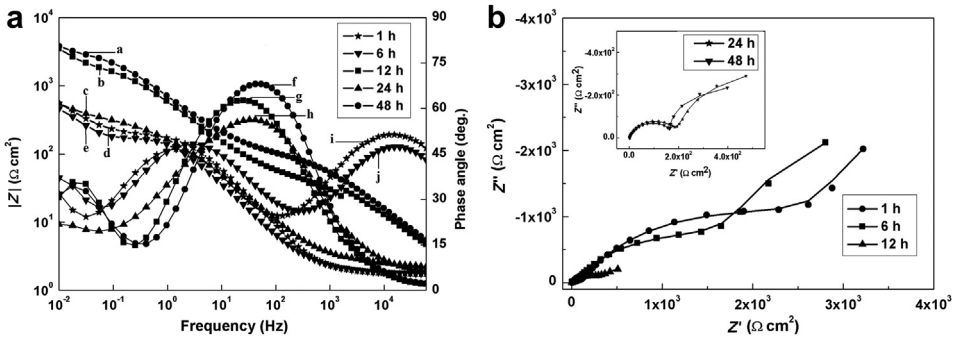

Fig. 7 (a) Bode and (b) Nyquist plots of Cu−Ni (90/10) alloy in seawater containing 10×10^{-6} sulphide in the absence of BTAH at 2200 r/min and at different immersion periods (temperature: 30 °C). a, b, c, d, e—frequency−Z curves; f, g, h, i, j—frequency−phase angle curves.

Table 5 Impedance parameters of Cu−Ni (90/10) alloy electrode in seawater containing 10×10^{-6} sulphide in the absence of BTAH at different hydrodynamic conditions and at different immersion periods (temperature: 30 °C)

Rotation speed (r/min)	Immersion period (h)	R_{ct} (kΩ cm^2)	CPE_{dl} (μF cm^{-2})	n_1	R_{film} (kΩ cm^2)	CPE_{film} (μF cm^{-2})	n_2
0	1	12.76	21.27	0.66	0.002	40.12	0.61
	6	7.21	24.10	0.64	0.002	48.29	0.61
	12	2.48	35.77	0.64	0.002	56.15	0.62
	24	0.89	47.91	0.64	0.001	62.54	0.63
	48	0.63	49.00	0.62	0.001	68.13	0.63
1000	1	6.89	12.41	0.61	0.139	25.84	0.61
	6	5.34	13.94	0.61	0.051	27.23	0.61
	12	1.95	17.86	0.61	0.002	30.16	0.61
	24	1.60	49.53	0.61	0.002	72.81	0.60
	48	0.62	54.76	0.60	0.001	74.47	0.60
2200	1	4.23	24.60	0.62	0.162	17.06	0.61
	6	2.40	27.14	0.62	0.114	30.61	0.61
	12	1.54	27.94	0.61	0.052	31.10	0.60
	24	0.16	142.2	0.60	0.002	153.0	0.60
	48	0.10	183.0	0.60	0.001	189.4	0.60

The Bode plots of Cu−Ni (90/10) alloy electrode immersed in seawater containing BTAH inhibitor at 0 r/min and at different immersion periods are shown in Fig. 8. These plots exhibit quite interesting features. The plots are so close to each other that they appear to be merged in the mid and high frequency regions. At all the immersion periods, the maxima of phase angle values are found to be close to 90°. This result reveals the protective nature of BTAH film on alloy surface[36−38]. The corresponding impedance parameters are calculated by using the equivalent circuit model shown in Fig. 3(b), with which the experimental data are fitted well. The results are given in Table 6. The R_{ct} and R_{film} values are enormously increased and CPE_{dl} and CPE_{film} values are drastically reduced in comparison with the values in the absence of inhibitor. The n_1 values are in the range of 0.94−0.98, which are nearly equal to 1. The increase in the maximum of phase angle to 90° and increase in n_1 values to 1 infer that BTAH film formed on alloy surface acts as an ideal capacitor.

It is of interest to investigate the effect of hydrodynamic condition of Cu−Ni (90/10) alloy working electrode on the efficiency of BTAH inhibitor. The Bode plots of Cu−Ni (90/10) alloy in seawater in the presence of 3.33 mmol/L BTAH at 1000 r/min are shown in Fig. 9. Even after 1 h immersion period, the impedance values are enormously increased in comparison with the values at 0 r/min. All the Bode plots are merged with each other at mid and high frequencies and show the maxima of phase angles close to 90°. Similar nature of Bode plots is also seen with a further increase in rotation speed to 2200 r/min as given in Fig. 10(a). The maxima of phase angles in Bode plots are much more broadened in a wide frequency region from 100 mHz to 10 kHz. These results infer the presence of a highly protective BTAH film on the alloy surface. The $|Z|$ *vs* f plots show linearity in the entire frequency region. The disappearance of Warburg impedance is noticed in the corresponding Nyquist plots as shown in Fig. 10(b). The diameter of semicircle is increased enormously with increasing immersion period. The impedance parameters of all these studies are given in Table 6. There is an enormous increase in both the R_{ct} and R_{film} values with increasing rotation speed. These results indicate that

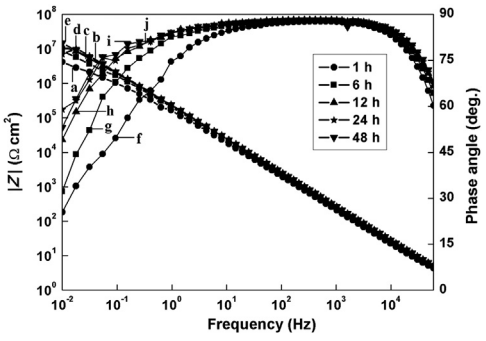

Fig. 8 Bode plots of Cu−Ni (90/10) alloy in seawater in the presence of 3.33 mmol/L BTAH at 0 r/min and at different immersion periods (temperature: 30 °C). a, b, c, d, e—frequency−Z curves; f, g, h, i, j—frequency−phase angle curves.

Table 6 Impedance parameters of Cu−Ni (90/10) alloy electrode in seawater in the presence of 3.33 mmol/L BTAH at different hydrodynamic conditions and at different immersion periods (temperature: 30 °C)

Rotation speed (r/min)	Immersion period (h)	R_{ct} (kΩ cm^2)	CPE_{dl} (μF cm^{-2})	n_1	R_{film} (kΩ cm^2)	CPE_{film} (μF cm^{-2})	n_2	IE (%)
0	1	1409	7.97	0.94	138.0	8.84	0.88	99.97
	6	3983	0.66	0.96	4866	5.96	0.90	99.98
	12	9387	0.61	0.98	9205	5.39	0.91	99.99
	24	13405	0.59	0.98	9247	4.07	0.95	99.98
	48	16772	0.57	0.98	10255	3.03	0.95	99.99
1000	1	566.3	1.47	0.88	144.8	1.61	0.88	99.28
	6	1757	0.41	0.90	684.2	0.43	0.89	99.62
	12	3692	0.13	0.93	700.7	0.36	0.94	97.05
	24	8169	0.10	0.97	1824	0.34	0.95	97.57
	48	18823	0.09	0.97	2495	0.31	0.96	98.93
2200	1	5135	0.08	0.92	366.3	0.17	0.87	99.97
	6	5865	0.05	0.92	1044	0.15	0.89	99.97
	12	15764	0.02	0.96	1415	0.08	0.91	99.22
	24	18277	0.02	0.98	1649	0.03	0.92	99.30
	48	19893	0.01	0.98	2122	0.03	0.92	99.37

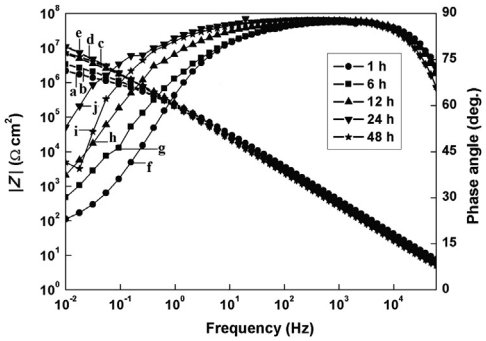

Fig. 9 Bode plots of Cu−Ni (90/10) alloy in seawater in the presence of 3.33 mmol/L BTAH at 1000 r/min and at different immersion periods (temperature: 30 °C). a, b, c, d, e—frequency−Z curves; f, g, h, i, j—frequency−phase angle curves.

hydrodynamic condition improves the protective nature of BTAH film. The R_{ct} and R_{film} values at 2200 r/min and after 48 h immersion period are found to be 19.89 and 2.12 MΩ cm^2, respectively. The corresponding n_1 and n_2 values are found to be 0.98 and 0.92, respectively. These results infer that BTAH film behaves as an ideal capacitor under hydrodynamic conditions also.

The Bode plots of Cu−Ni (90/10) alloy in seawater containing 10×10^{-6} sulphide and 3.33 mmol/L BTAH at 0 r/min are shown in Fig. 11. These plots also show a similar nature as observed in case of seawater containing BTAH, but no sulphide ions. With increasing rotation speed, the phase angle Bode plots show broadening of the maxima of phase angles as well as increase in maxima close to 90° (Figs. 12 and 13(a)). The Warburg impedance in Nyquist plots is completely absent at all rotation speeds and immersion periods. As a typical example, the Nyquist plots at 2200 r/min only are shown in Fig. 13(b). The impedance parameters of all these studies are given in Table 7. At 2200 r/min, the R_{ct} value after 48 h immersion period is found to be 27.48 MΩ cm^2, which is higher than that in the case of seawater + BTAH. This result indicates that the protective nature of BTAH film is still better in seawater containing 10×10^{-6} sulphide. The impedance studies infer that BTAH is an excellent inhibitor for Cu−Ni (90/10) alloy in seawater and seawater containing 10×10^{-6} sulphide under both static and hydrodynamic conditions.

3.3. Potentiodynamic polarization studies

The potentiodynamic polarization curves of Cu−Ni (90/10) alloy in seawater in the absence of any inhibitor at both 0 and 2200 r/min are shown in Fig. 14. The corresponding corrosion parameters are given in Table 8. At 0 r/min, the corrosion current density is decreased with increasing immersion period. The decrease in i_{corr} infers that the oxide film becomes more protective. An active−passive transition followed by a short passive region is observed in the anodic curve. There is breakdown of

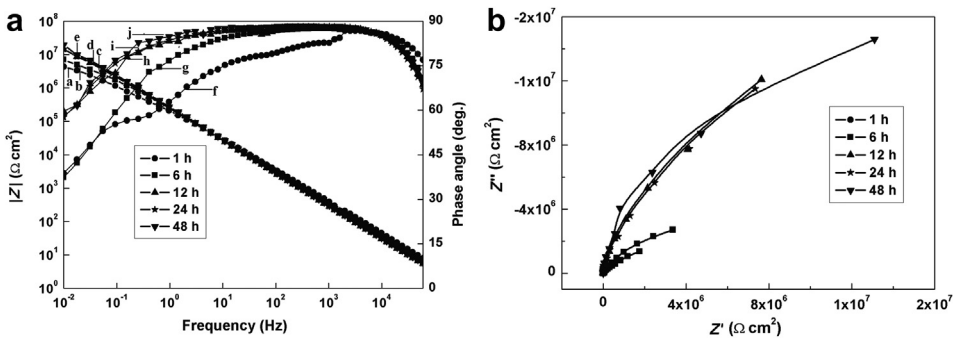

Fig. 10 (a) Bode and (b) Nyquist plots of Cu−Ni (90/10) alloy in seawater in the presence of 3.33 mmol/L BTAH at 2200 r/min and at different immersion periods (temperature: 30 °C). a, b, c, d, e—frequency−Z curves; f, g, h, i, j—frequency−phase angle curves.

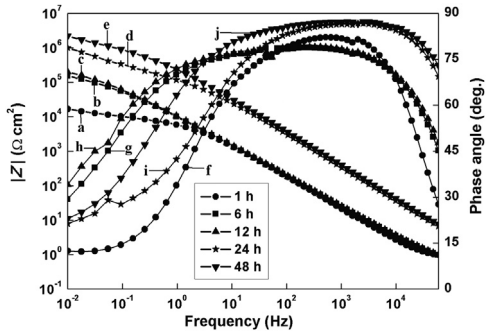

Fig. 11 Bode plots of Cu−Ni (90/10) alloy in seawater containing 10×10^{-6} sulphide in the presence of 3.33 mmol/L BTAH at 0 r/min and at different immersion periods (temperature: 30 °C). a, b, c, d, e—frequency−Z curves; f, g, h, i, j—frequency−phase angle curves.

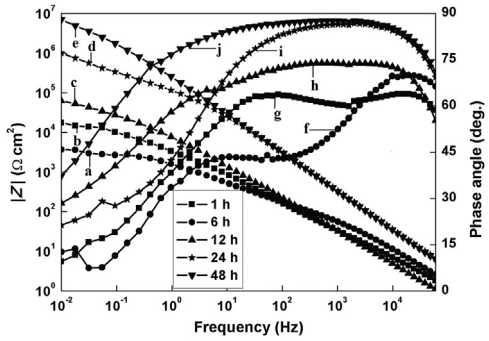

Fig. 12 Bode plots of Cu−Ni (90/10) alloy in seawater containing 10×10^{-6} sulphide in the presence of 3.33 mmol/L BTAH at 1000 r/min and at different immersion periods (temperature: 30 °C). a, b, c, d, e—frequency−Z curves; f, g, h, i, j—frequency−phase angle curves.

passivity followed by well-defined hysteresis loop. The E_{corr} values are shifted towards less negative potentials with increasing rotation speed from 0 to 2200 r/min. The same active−passive regions are also seen in the case of 2200 r/min. However, at 2200 r/min, the i_{corr} values are increased slightly with increasing immersion period from 1 to 48 h (Table 8). Whereas, the R_{ct} values are increased with increasing immersion period under hydrodynamic conditions (0−2200 r/min) also (Table 4). These observations can be explained as follows. The electrochemical impedance studies are carried out at open circuit potentials with only ±5 mV of amplitude. Thus, the electrode is not deliberately polarized to anodic potentials. Under this condition of the electrode, at 2200 r/min, with increasing immersion time, the protective nature of Cu_2O film is increased, which is evidenced by an increase in R_{ct} value. De Sanchez and Schiffrin[26] reported an increase in R_{ct} value with increasing rotation speed and also with increasing immersion time at a given rotation speed for Cu−Ni (90/10) alloy in seawater. But, in potentiodynamic polarization studies at 2200 r/min, the electrode is polarized starting from −0.7 V to +0.7 V *vs* Ag/AgCl/1.0 mol/L KCl. Therefore, because of the combination of higher anodic potentials applied and also high rotation speed of the electrode *viz* 2200 r/min, there is dissolution of the passive film with increasing immersion time and hence the observation of slight increase in i_{corr} with increasing immersion time. The Cu_2O film loss occurred by localized impingement attack by chloride, which facilitated dissolution[18]. Similar results of increase of i_{corr} values with immersion time under hydrodynamic condition of Cu−Ni (90/10) alloy in artificial seawater was reported by Mansfeld et al.[39]. They have found an increase in i_{corr} values with increasing rotation speed and immersion time at a given rotation speed.

In the presence of seawater containing 10×10^{-6} sulphide ions, the E_{corr} values at 0 r/min (Fig. 15) are shifted towards more negative potentials in comparison with seawater containing no sulphide ions. The corrosion parameters are given in Table 9. The shift in E_{corr} suggests that the alloy has greater tendency towards corrosion in the presence of sulphide ions[40−42]. An active−passive transition followed by a short passive region is observed in anodic curve. There is breakdown of passivity followed by well-defined hysteresis loop. The entire phenomenon is interpreted by localized attack of sulphide ions on the alloy surface[43,44]. The corrosion current density after 48 h immersion period is found to be 2.5 μA cm^{-2}, which is higher than that in the absence of sulphide ions. Under hydrodynamic condition at 2200 r/min of the electrode, the i_{corr} values are enormously increased. After 48 h immersion period, the i_{corr} value is found to be 37.1 μA cm^{-2}, which is far higher than that in the absence of sulphide ions. The active−passive regions followed by hysteresis loop are also seen. These results reveal that the corrosion damage occurring on Cu−Ni (90/10) alloy under hydrodynamic conditions is more than that under static conditions.

The potentiodynamic polarization curves of Cu−Ni (90/10) alloy in seawater in the presence of 3.33 mmol/L BTAH at 0 and 2200 r/min are shown in Fig. 16. The corresponding corrosion parameters are given in Table 10. At 0 r/min, the E_{corr} is shifted

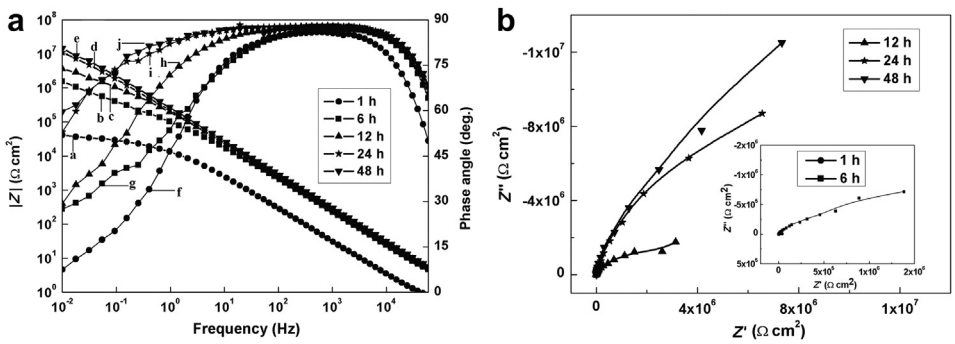

Fig. 13 (a) Bode and (b) Nyquist plots of Cu−Ni (90/10) alloy in seawater containing 10×10^{-6} sulphide in the presence of 3.33 mmol/L BTAH at 2200 r/min and at different immersion periods (temperature: 30 °C). a, b, c, d, e—frequency−Z curves; f, g, h, i, j—frequency−phase angle curves.

Table 7 Impedance parameters of Cu−Ni (90/10) alloy electrode in seawater containing 10×10^{-6} sulphide in the presence of 3.33 mmol/L BTAH at different hydrodynamic conditions and at different immersion periods (temperature: 30 °C)

Rotation speed (r/min)	Immersion period (h)	R_{ct} (kΩ cm^2)	CPE_{dl} (μF cm^{-2})	n_1	R_{film} (kΩ cm^2)	CPE_{film} (μF cm^{-2})	n_2	IE (%)
0	1	32.56	11.20	0.89	5.55	21.49	0.84	45.46
	6	168.7	10.06	0.92	68.19	13.40	0.84	95.73
	12	249.8	8.49	0.94	95.06	11.83	0.85	99.01
	24	756.0	6.67	0.96	117.0	7.87	0.88	99.88
	48	2322	5.40	0.96	460.5	6.83	0.88	99.97
1000	1	22.47	12.78	0.87	6.66	11.60	0.81	69.34
	6	53.39	4.13	0.90	11.66	8.64	0.82	89.98
	12	91.98	2.06	0.92	20.17	5.00	0.88	97.88
	24	672.7	0.10	0.95	378.0	4.46	0.93	99.76
	48	6972	0.03	0.98	680.0	0.44	0.96	99.99
2200	1	31.42	5.01	0.90	0.22	30.66	0.90	86.54
	6	939.4	0.09	0.92	82.88	0.69	0.92	99.74
	12	4172	0.05	0.98	354.9	0.60	0.95	99.96
	24	21189	0.04	0.99	1812	0.43	0.96	99.99
	48	27478	0.04	0.99	2520	0.39	0.97	99.99

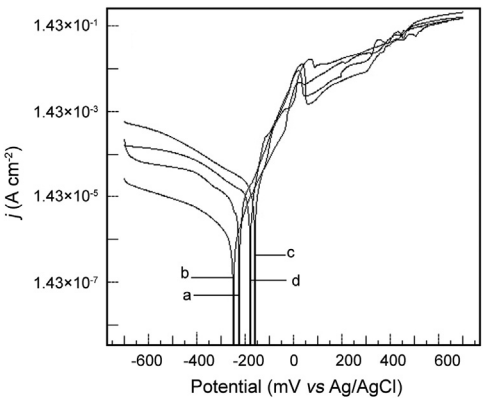

Fig. 14 Potentiodynamic polarization curves of Cu−Ni (90/10) alloy in seawater in the absence of BTAH at 0 r/min (a − 1 h, b − 48 h) and 2200 r/min (c − 1 h, d − 48 h) (temperature: 30 °C).

towards less negative potentials in comparison with seawater containing no BTAH. The i_{corr} values are significantly reduced even at 1 h immersion period and they are decreased further with increasing immersion period to 48 h. Another significant feature is complete absence of active−passive transition followed by hysteresis loop in the anodic region. The anodic region up to +650 mV *vs* Ag/AgCl is stable. This result infers the presence of a protective BTAH film on the alloy surface, which is quite stable. At 2200 r/min, the i_{corr} values are slightly higher than those at 0 r/min. Nevertheless, these values are far lower than those in the absence of BTAH. The anodic region up to +650 mV *vs* Ag/AgCl is quite stable. There is complete absence of active−passive transition followed by hysteresis loop. Both the anodic Tafel slope and cathodic Tafel slope are shifted in the presence of inhibitor. Hence, it can be inferred that BTAH functions as a mixed inhibitor. The inhibition efficiencies are found to be in the range of 99.92%−98.90%.

The potentiodynamic polarization curves of the alloy in seawater containing sulphide ions in the presence of BTAH at both 0 and 2200 r/min are shown in Fig. 17. The nature of the plots is similar to those observed in seawater containing BTAH, but no sulphide ions. The corrosion parameters are given in Table 11. The anodic region up to +450 mV *vs* Ag/AgCl is stable. There is complete absence of active−passive transition followed by hysteresis loop. The results infer that BTAH functions as an excellent mixed inhibitor with inhibition efficiencies in the range of 99.9%−99.6% even in seawater containing sulphide ions under static as well as hydrodynamic conditions.

3.4. Cyclic voltammetric studies

The cyclic voltammograms of Cu−Ni (90/10) alloy in seawater in the absence of BTAH in the potential range −1.0 V to +1.0 V *vs* Ag/AgCl at 0 r/min and at two immersion periods (1 and 48 h) are shown in Fig. 18(a) and (b), respectively. At 1 h immersion period, in the first cycle, the forward sweep exhibits only one anodic peak at +250 mV *vs* Ag/AgCl. In the reverse sweep also only one cathodic peak is observed due to corresponding reduction reaction. In the second cycle, the forward sweep exhibits two anodic peaks. In the reverse sweep also, two cathodic peaks are observed due to corresponding reduction reactions[45−47]. Both the anodic and cathodic peak currents are increased to some extent in the second cycle. After 48 h immersion, in the first cycle, no anodic peak is observed up to +400 mV *vs* Ag/AgCl and the current remains constant in this region. This is because of the presence of mature Cu_2O film on alloy surface, which protects the alloy from corrosion to some extent. After +400 mV *vs* Ag/AgCl, the current values are increased

Table 8 Corrosion parameters of Cu−Ni (90/10) alloy electrode obtained by potentiodynamic polarization studies in seawater in the absence of BTAH under static as well as hydrodynamic conditions and at different immersion periods (temperature: 30 °C)

Rotation speed (r/min)	Immersion period (h)	E_{corr} (mV)	i_{corr} (μA cm^{-2})	β_c (mV/decade)	β_a (mV/decade)
0	1	−222.8	6.5	−149.0	63.2
	48	−255.5	1.2	−137.0	65.2
2200	1	−160.7	10.7	−78.1	46.7
	48	−174.1	11.3	−171.0	36.3

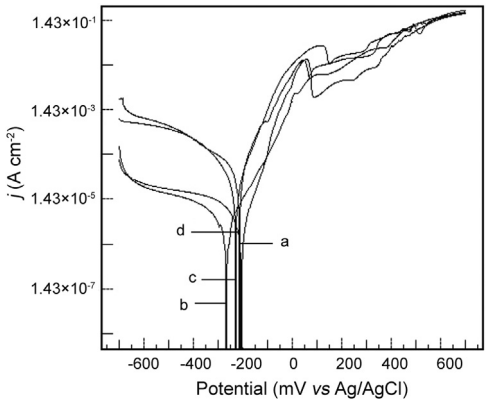

Fig. 15 Potentiodynamic polarization curves of Cu−Ni (90/10) alloy in seawater containing 10×10^{-6} sulphide in the absence of BTAH at 0 r/min (a − 1 h, b − 48 h) and 2200 r/min (c − 1 h, d − 48 h) (temperature: 30 °C).

Table 9 Corrosion parameters of Cu−Ni (90/10) alloy electrode obtained by potentiodynamic polarization studies in seawater containing 10×10^{-6} sulphide in the absence of 3.33 mmol/L BTAH under static as well as hydrodynamic conditions and at different immersion periods (temperature: 30 °C)

Rotation speed (r/min)	Immersion period (h)	E_{corr} (mV)	i_{corr} (μA cm^{-2})	β_c (mV/decade)	β_a (mV/decade)
0	1	−201.3	3.2	−143.0	61.2
	48	−272.0	2.5	−123.0	89.3
2200	1	−223.0	19.3	−102.0	52.9
	48	−210.2	37.1	−135.0	56.2

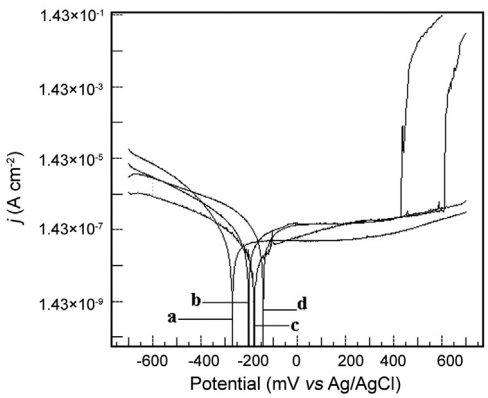

Fig. 16 Potentiodynamic polarization curves of Cu−Ni (90/10) alloy in seawater in the presence of BTAH at 0 r/min (a − 1 h, b − 48 h) and 2200 r/min (c − 1 h, d − 48 h) (temperature: 30 °C).

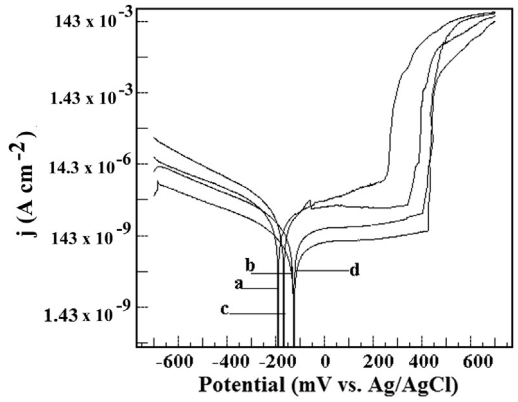

Fig. 17 Potentiodynamic polarization curves of Cu−Ni (90/10) alloy in seawater containing 10×10^{-6} sulphide in the presence of BTAH at 0 r/min (a − 1 h, b − 48 h) and 2200 r/min (c − 1 h, d − 48 h) (temperature: 30 °C).

because of the breakdown of passivity. In the reverse sweep of first cycle and forward sweep of second cycle, the same behaviour as observed in the case of 1 h is noticed. Similar behaviour is also seen at 2200 r/min (Fig. 19(a) and (b)). The anodic and cathodic peak currents are slightly less in the case of 2200 r/min in comparison with 0 r/min. This indicates the formation of Cu_2O film on alloy surface under hydrodynamic conditions also. The oxidation of Cu−Ni (90/10) alloy occurs in seawater *via* dissolution of Cu. Two anodic peaks are observed, which correspond to reactions shown in Eqs. (4) and (5), respectively[19].

$$Cu + Cl^- \Leftrightarrow CuCl + 1e^- \quad (4)$$

$$CuCl + Cl^- \Leftrightarrow CuCl_2^- \quad (5)$$

In seawater containing sulphide at 0 r/min (Fig. 20(a) and (b)), in the first cycle itself, there is presence of two anodic and cathodic peaks. This indicates active dissolution of Cu into seawater environment in the presence of sulphide ions. The passive region which is observed in seawater in the absence of sulphide ions up to +400 mV *vs* Ag/AgCl is not seen in seawater containing sulphide. This infers that there is adverse effect of sulphide ions on the formation of Cu_2O film. Similar nature of CV is seen at 2200 r/min (Fig. 21(a) and (b)) also. Nevertheless, in the presence of sulphide, both the anodic and cathodic peak currents are increased with increasing rotation speed. In seawater containing sulphide, hydrosulfide (HS^-) ions are known to promote corrosion of alloy[26,40]. The first step is an initial adsorption process, which is shown in Eq. (6),

$$HS^-_{(aq)} + Cu \Leftrightarrow HS^-: Cu \quad (6)$$

where HS^-:Cu is adsorbed sulphide species on the Cu−Ni (90/10) alloy surface. This adsorbed species catalyzes the anodic dissolution reaction as shown in Eq. (7)[21],

Table 10 Corrosion parameters of Cu−Ni (90/10) alloy electrode obtained by potentiodynamic polarization studies in seawater in the presence of 3.33 mmol/L BTAH under static as well as hydrodynamic conditions and at different immersion periods (temperature: 30 °C)

Rotation speed (r/min)	Immersion period (h)	E_{corr} (mV)	i_{corr} (μA cm^{-2})	β_c (mV/decade)	β_a (mV/decade)	IE (%)
0	1	−271.4	0.025	−77.3	87.0	99.6
	48	−200.9	0.013	−39.2	68.4	98.9
2200	1	−181.0	0.033	−61.7	83.2	99.9
	48	−138.5	0.009	−74.6	82.8	99.7

Table 11 Corrosion parameters of Cu−Ni (90/10) alloy electrode obtained by potentiodynamic polarization studies in seawater containing 10×10^{-6} sulphide in the presence of 3.33 mmol/L BTAH under static as well as hydrodynamic conditions and at different immersion periods (temperature: 30 °C)

Rotation speed (r/min)	Immersion period (h)	E_{corr} (mV)	i_{corr} (μA cm^{-2})	β_c (mV/decade)	β_a (mV/decade)	IE (%)
0	1	−192.0	0.133	−80.0	100.0	95.8
	48	−127.8	0.011	−44.6	59.4	99.6
2200	1	−171.3	0.119	−55.3	82.3	99.4
	48	−129.1	0.052	−74.9	123.0	99.9

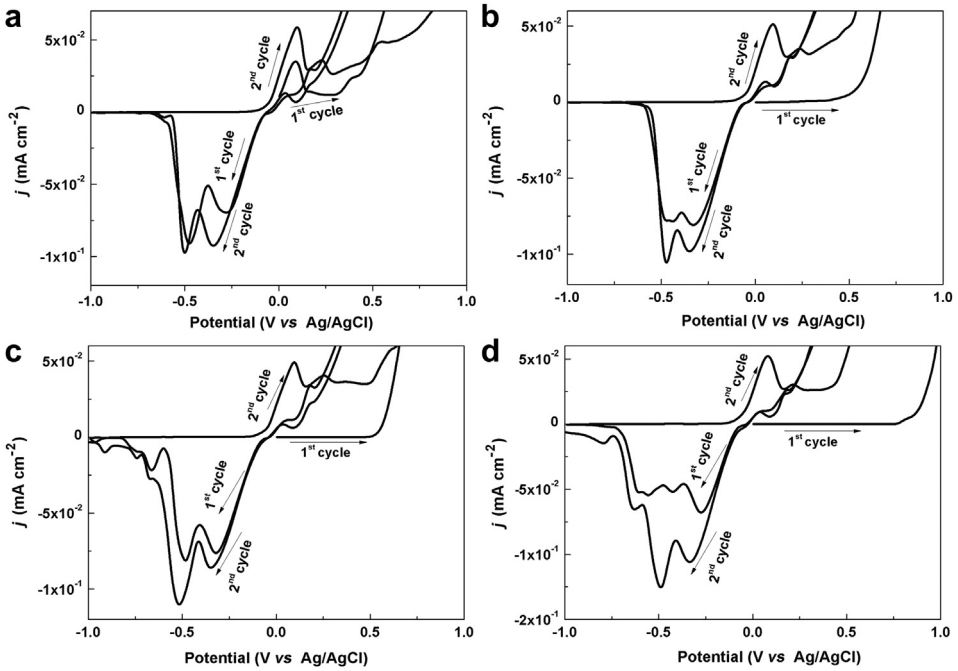

Fig. 18 Cyclic voltammograms of Cu−Ni (90/10) alloy in seawater at 0 r/min in the absence (a − 1 h, b − 48 h) and presence (c − 1 h, d − 48 h) of 3.33 mmol/L BTAH (temperature: 30 °C).

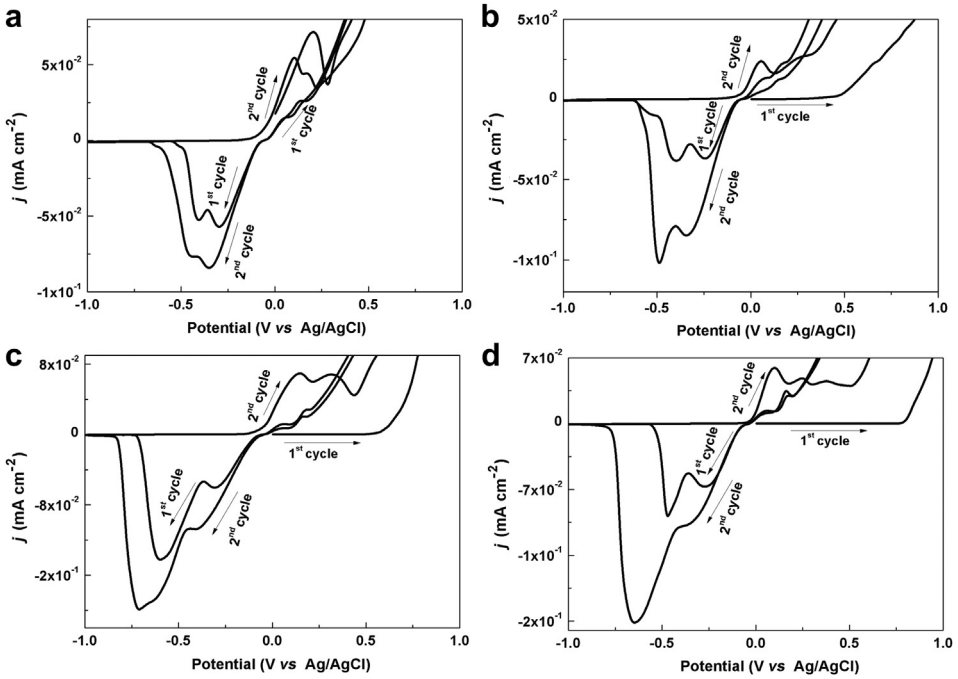

Fig. 19 Cyclic voltammograms of Cu−Ni (90/10) alloy in seawater at 2200 r/min in the absence (a − 1 h, b − 48 h) and presence (c − 1 h, d − 48 h) of 3.33 mmol/L BTAH (temperature: 30 °C).

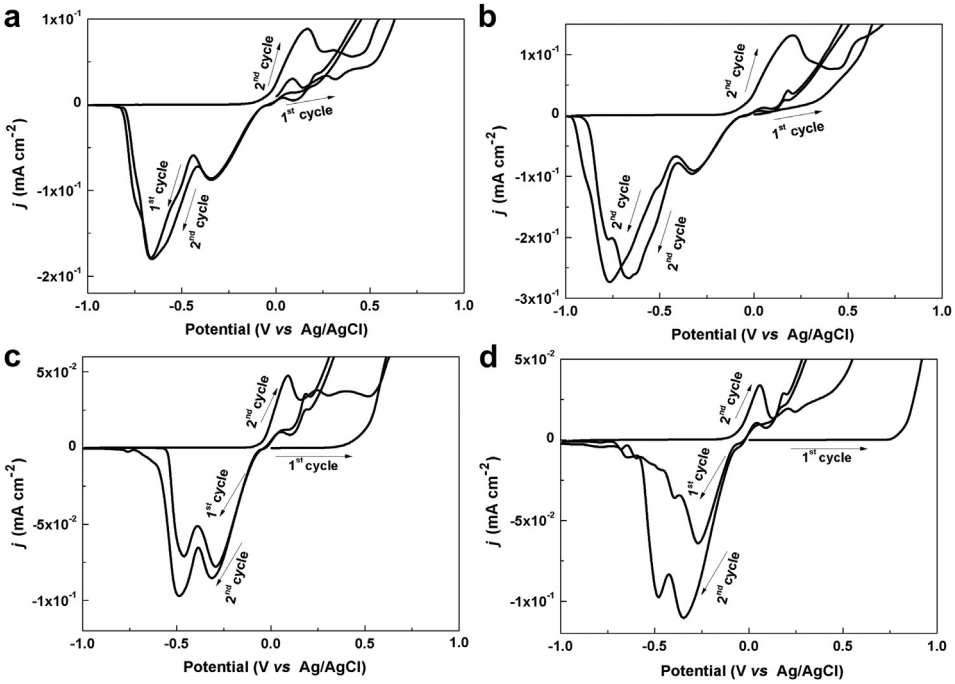

Fig. 20 Cyclic voltammograms of Cu−Ni (90/10) alloy in seawater containing 10×10^{-6} sulphide at 0 r/min in the absence (a − 1 h, b − 48 h) and presence (c − 1 h, d − 48 h) of 3.33 mmol/L BTAH (temperature: 30 °C).

$$HS^- : Cu \Leftrightarrow CuS + H^+ + 2e^- \quad (7)$$

$$1/2O_2 + H_2O + 2e^- \rightarrow 2OH^- \quad (8)$$

The resulting sulfide scale (CuS and Cu_2S), as well as dissolved sulfide, catalyze the partial anodic reaction (Eq. (7)) and also the partial cathodic reaction, which involves the reduction of oxygen as shown in Eq. (8),

The overall corrosion reaction is the sum of the two partial reactions (Eqs. (7) and (8)) which can be represented by the Eq. (9),

$$HS^- : Cu + 1/2O_2 \rightarrow CuS + OH^- \quad (9)$$

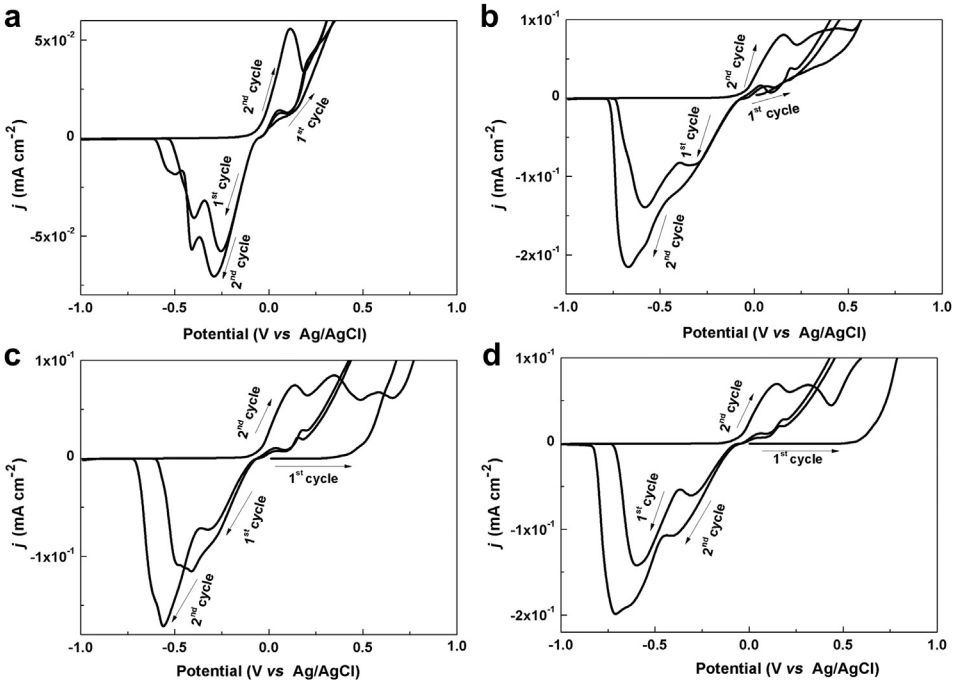

Fig. 21 Cyclic voltammograms of Cu−Ni (90/10) alloy in seawater containing 10×10^{-6} sulphide at 2200 r/min in the absence (a − 1 h, b − 48 h) and presence (c − 1 h, d − 48 h) of 3.33 mmol/L BTAH (temperature: 30 °C).

In the presence of 3.33 mmol/L BTAH, at 0 r/min (Fig. 18(c) and (d)), even at 1 h immersion period, there are no anodic peaks. The current remains constant up to +750 mV *vs* Ag/AgCl. This indicates the presence of protective BTAH film on the alloy surface, which prevents the dissolution of Cu. After 48 h immersion period, the protective nature of the film is increased up to +1.0 V *vs* Ag/AgCl at 0 r/min and up to +850 mV *vs* Ag/AgCl at 2200 r/min (Fig. 19(c) and (d)). Similar behaviour is also seen in seawater containing sulphide at both 0 (Fig. 20(c) and (d)) and 2200 r/min (Fig. 21(c) and (d)). These results reveal that the protective BTAH film protects Cu−Ni (90/10) alloy from corrosion even in seawater containing sulphide ions under static as well as hydrodynamic conditions. In the presence of BTAH[21], there is chemisorption of BTAH on the alloy surface followed by the formation of polymeric complex, as shown in Eqs. (10) and (11), respectively,

$$\mathrm{BTAH_{(aq)} + Cu \rightarrow BTAH : Cu\ (Chemisorption\ step)} \quad (10)$$

$$n\mathrm{BTAH} + n\mathrm{Cu^{+}} \rightarrow [\mathrm{Cu(1)BTA}]_n + n\mathrm{H^{+}}$$
$$\mathrm{(Polymeric\ complex\ formation)} \quad (11)$$

4. Conclusions

(1) All the three electrochemical methods reveal that 1,2,3-benzotriazole is proved to be an excellent inhibitor for Cu−Ni (90/10) alloy in synthetic seawater and seawater containing sulphide ions under static as well as hydrodynamic conditions under laminar flow.

(2) Electrochemical impedance studies show that the presence of BTAH molecules in both seawater and sulphide containing seawater increases the charge transfer resistance and the film resistance of the Cu−Ni (90/10) alloy enormously even at 2200 r/min. The broadening of the maximum of phase angle and increase in *n* value close to 1 in the presence of BTAH infer that BTAH acts as an ideal capacitor under both static and hydrodynamic conditions.

(3) Potentiodynamic polarization studies give valuable information regarding the anodic behaviour of Cu−Ni (90/10) alloy in the absence and presence of BTAH, which is proved to be a mixed inhibitor. Under hydrodynamic conditions also, BTAH considerably shifts the corrosion potential to less negative values and greatly decreases the corrosion current density. The BTAH film protects the alloy even when it is anodically polarized up to +650 mV *vs* Ag/AgCl under static as well as hydrodynamic conditions.

(4) Cyclic voltammeric studies show the stability of the protective film under hydrodynamic conditions even at higher anodic potentials such as +850 mV *vs* Ag/AgCl.

Acknowledgements

The authors are grateful to Naval Research Board (NRB), Govt. of India and Rajiv Gandhi National Fellowship (RGNF), UGC, Govt. of India for giving the financial assistance.

REFERENCES

[1] L. Kenworthy, Trans. Inst. Marine. Eng. 77 (1965) 149−160.
[2] B. Todd, Marine Applications of Copper−Nickel Alloys, Section 2: Materials Selection for High Reliability Seawater Systems, Technical Report, Copper Development Association, Potters Bar, UK, 1998.
[3] A Working Party Report, Illustrated Case Histories of Marine Corrosion, The Institute of Metals, London, 1990.
[4] S. Cere, M. Vazquez, J. Mater. Sci. Lett. 21 (2002) 493−495.
[5] J.O.M. Bockris, B.T. Rubin, A. Despic, B. Lovrecek, Electrochim. Acta 17 (1972) 973−999.
[6] R.F. North, M.J. Pryor, Corros. Sci. 10 (1970) 297−311.
[7] J.F. Bates, J.M. Popplewell, Corrosion 31 (1975) 269−275.
[8] J.P. Gudas, H.P. Hack, Corrosion 35 (1979) 67−73.
[9] E.D. Mor, A.M. Beccaria, Brit. Corros. J. 10 (1975) 33−38.
[10] A.A. Hashem, P.G. Caceres, W.T. Riad, H.M. Shalaby, Corrosion 51 (1995) 331−342.
[11] R.F. Schmidt, F.L. Riddell, Trans. Am. Foundry. Soc. 73 (1965) 471−474.
[12] T.J. Glover, Mater. Perform. 27 (1988) 51.
[13] A.H. Tuthill, Mater. Perform. 26 (1987) 12.
[14] G. Kear, D.B. Barker, F.C. Walsh, Corros. Sci. 46 (2004) 109−135.
[15] B. Todd, P.A. Lovett, Marine Engineering Practice: Selecting Materials for Seawater Systems, vol. 1, part 10, The Institute of Marine Engineers, London, UK, 1974.
[16] K.D. Efird, D.B. Anderson, Mater. Perform. 14 (1975) 37.
[17] G. Kear, B.D. Barker, K.R. Stokes, F.C. Walsh, Corrosion 65 (2009) 24−36.
[18] M.R.F. Hurtado, P.T.A. Sumodjo, A.V. Benedetti, Electrochim. Acta 48 (2003) 2791−2798.
[19] M.E. Walton, P.A. Brook, Corros. Sci. 17 (1977) 317−326.
[20] R. Babic, M. Metikos-Hukovic, M. Loncar, Electrochim. Acta 44 (1999) 2413−2421.
[21] N.K. Allam, E.A. Ashour, H.S. Hegazy, B.E. El-Anadouli, B.G. Ateya, Corros. Sci. 47 (2005) 2280−2292.
[22] J.M. Maciel, S.M.L. Agostinho, J. Appl. Electrochem. 30 (2000) 981−985.
[23] B.V. Appa Rao, K. Chaitanya Kumar, ISRN Corros. 2013 (2013) 1−22.
[24] J.P. Bidwell, S. Spotte, Simulated Seawaters: Formulas and Methods, Jones & Bartlett Publishers, Boston, 1985.
[25] A.L. Bacarella, J.C. Griess, J. Electrochem. Soc. 120 (1973) 459−465.
[26] S.R. De Sanchez, D.J. Schiffrin, Corros. Sci. 22 (1982) 585−607.
[27] S.J. Yuan, S.O. Pehkonen, Corros. Sci. 49 (2007) 1276−1304.
[28] F. Bentiss, M. Lagrenee, M. Traisnel, J.C. Hornez, Corros. Sci. 41 (1999) 789−803.
[29] Y.S. Tan, M.P. Srinivasan, S.O. Pehkonen, Y.M. Simon Chooi, Corros. Sci. 48 (2006) 840−862.
[30] X. Wu, H. Ma, S. Chen, Z. Xu, A. Sui, J. Electrochem. Soc. 146 (1999) 1847−1853.
[31] C. Kato, B.G. Ateya, J.E. Castle, H.W. Pickering, J. Electrochem. Soc. 127 (1980) 1897−1903.
[32] Y.Z. Wang, A.M. Beccaria, G. Poggi, Corros. Sci. 36 (1994) 1277−1288.
[33] P. Druska, H.H. Strehblow, S. Golledge, Corros. Sci. 38 (1996) 835−851.
[34] J.M. Popplewell, R.J. Hart, J.A. Ford, Corros. Sci. 13 (1973) 295−309.
[35] R.G. Blundy, M.J. Pryor, Corros. Sci. 12 (1972) 65−75.
[36] G.W. Poling, Corros. Sci. 10 (1970) 359−370.
[37] J.H. Chen, Z.C. Lin, S. Chen, L.H. Nie, S.Z. Yao, Electrochim. Acta 43 (1998) 265−274.
[38] F. Mansfeld, T. Smith, Corrosion 29 (1973) 105−107.
[39] F. Mansfeld, G. Liu, H. Xiao, C.H. Tsai, B.J. Little, Corros. Sci. 36 (1994) 2063−2095.
[40] J.N. Al-Hajji, M.R. Reda, J. Electrochem. Soc. 142 (1995) 2944−2953.
[41] J.N. Al-Hajji, M.R. Reda, J. Electrochem. Soc. 141 (1994) 1432−1439.
[42] J.N. Al-Hajji, M.R. Reda, Corros. Sci. 34 (1993) 163−177.
[43] G. Huang, H.Y. Chan, H.H.P. Fang, J. Electrochem. Soc. 151 (2004) B434−B439.
[44] D.J. Schiffrin, S.R. De Sanchez, Corrosion 41 (1985) 31−38.
[45] S.M. Wilhelm, Y. Tanizawa, C.Y. Liu, N. Hackerman, Corros. Sci. 22 (1982) 791−805.
[46] H.H. Strehblow, B. Titze, Electrochim. Acta 25 (1980) 839−850.
[47] A. Aruchamy, Fujishima, J. Electroanal. Chem. 266 (1989) 397−408.